MODELLING IN THE NONLINEAR BEHAVIOUR OF LAMINATED COMPOSITE PLATES

DOMENICO BRUNO GIUSEPPE SPADEA

GIACINTO PORCO

Department of Structures, University of Calabria - Cosenza, Italy.

Third International Conference on Biaxial/Multiaxial Fatigue, April 3-6, 1989 Stuttgart, FRG.

SUMMARY

The nonlinear behaviour of laminated composite plates is studied using a shear deformable plate theory accounting for transverse shear (as in Reissner-Mindlin's thick plate theory) and large displacements (as in von Karman's theory). The analysis is devoted to the investigation of nonlinear bending and buckling of composite plates, and delamination in plates with initial bonding defects. Also given are some numerical results for rectangular plates, obtained via finite elements, under various boundary conditions and loadings, and for different stacking and orientation of layers and material properties.

INTRODUCTION

Laminated composite plates find wide application in the aerospace industry due to the their high stiffness-to-weight ratio, and to the capability of the anisotropic properties to be tailored by varying the fiber orientation and stacking sequence.

Because of the increasing use of fiber reinforced composite laminates in engineering structures, studies on mechanical behaviour of composite plates are receiving a great deal of attention.

Due to the high ratio of in-plane modulus to transverse shear modulus, the shear deformation effects are more pronunced in the composite laminates than in the isotropic plates. The classical thin plate theory, based on the

Kirchhoff-Love assumption that normals to the mid-surface before deformation remain straight and normal to the mid-surface after deformation, is not adequate for the flexural analysis of moderately thick laminates [1÷4].

In this work an analysis on the nonlinear behaviour of laminated composite plates is developed using a shear deformable plate theory [5÷9] which also includes nonlinear terms in the strain-displacement relationship. In particular, the influence of the anisotropic properties of the laminate on the nonlinear bending and buckling behaviour [10-11-14] of sandwich plates is investigated.

In addition, the delamination failure in laminated composite plates [12-15-16] with initial bonding defects between layers is studied both by an analytical approach based on the fracture mechanics results and by a finite element approach, in which adhesion between layers is modelled as unilateral springs.

PLATE MODEL

With reference to Fig. 1, a laminated plate is examined, with n arbitrarily oriented anisotropic layers; the total thickness of the plate is h. The origin of the coordinate system (x,y) is taken in the middle plane Ω of the plate with the z-axis perpendicular to it.

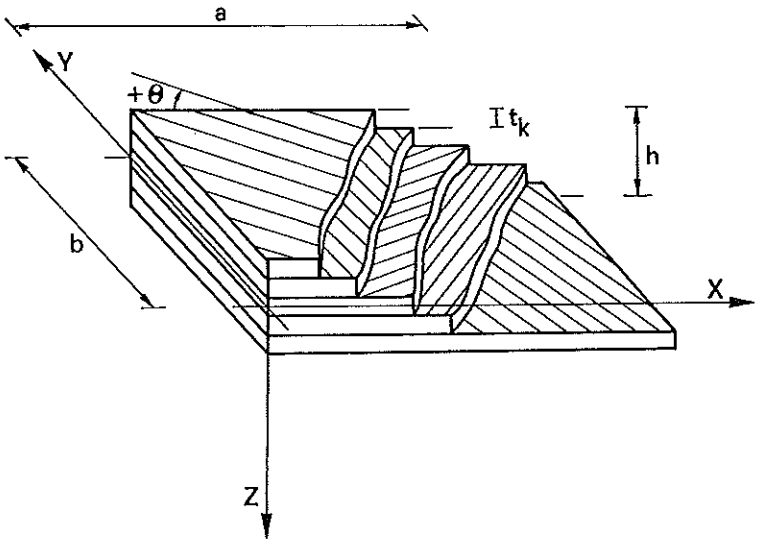

Fig. 1 - Multilayered plate.

The displacement field is assumed to be of the form:

$$u_x(x,y,z) = u(x,y) + z\psi_x(x,y) \ , \tag{1a}$$

$$u_y(x,y,z) = v(x,y) + z\psi_y(x,y) \ , \tag{1b}$$

$$u_z(x,y,z) = w(x,y) \ , \tag{1c}$$

where u_x, u_y, u_z are the displacements in the directions x,y and z, respectively; u,v,w are the corresponding midplane displacements, and ψ_x, ψ_y are the bending slopes in the xz and yz planes.

Assuming that the plate is moderately thick and strains are much smaller than rotations, the nonlinear strain-displacement relations can be taken as:

$$\varepsilon_1 \equiv \varepsilon_{xx} = u_{,x} + \frac{1}{2} w_{,x}^2 + z\psi_{x,x} = \varepsilon_1^\circ + z\chi_1 \tag{2a}$$

$$\varepsilon_2 \equiv \varepsilon_{yy} = v_{,y} + \frac{1}{2} w_{,y}^2 + z\psi_{y,y} = \varepsilon_2^\circ + z\chi_2 \tag{2b}$$

$$\varepsilon_6 \equiv 2\varepsilon_{xy} = u_{,y} + v_{,y} + w_{,x}\, w_{,y} + z(\psi_{x,y} + \psi_{y,x}) = \varepsilon_6^\circ + z\chi_6 \tag{2c}$$

$$\varepsilon_3 \equiv \varepsilon_{zz} = \psi_x^2 + \psi_y^2 \ , \ \varepsilon_4 \equiv 2\varepsilon_{xz} = \psi_x + w_{,x} \ , \ \varepsilon_5 \equiv 2\varepsilon_{yz} = \psi_y + w_{,y} \tag{2d}$$

Since the constitutive relations are based on the plane-stress assumption, the total potential energy of the plate, in the absence of body forces and neglecting both body moments and surface shearing forces, is given by:

$$\Pi = \frac{1}{2}\int_\Omega (N_1\varepsilon_1 + N_2\varepsilon_2^\circ + N_6\varepsilon_6^\circ + M_1\chi_1 + M_2\chi_2 + M_6\chi_6 + Q_4\varepsilon_4 + Q_5\varepsilon_5)d\Omega - \int_\Omega qw \ d\Omega +$$

$$- \int_{C_1} \bar{N}_n u_n ds - \int_{C_2} \bar{N}_n u_{ns} ds - \int_{C_3} \bar{M}_n \psi_n ds - \int_{C_4} \bar{M}_s \psi_s \ ds - \int_{C_5} \bar{Q}_n w \ ds \tag{3}$$

where N_1, M_1, etc., are the stress and moment resultants, given by:

$$N_i = \int_{-h/2}^{h/2} \sigma_i \ dz \ , \quad M_i = \int_{-h/2}^{h/2} \sigma_i \ z \ dz \ , \quad Q_4 = \int_{-h/2}^{h/2} \sigma_4 \ dz \ , \ Q_5 = \int_{-h/2}^{h/2} \sigma_5 \ dz \tag{4}$$

Here, $\sigma_i^{(k)}$ (i=1,2,6) denote the in plane stress components and z_k and $z_{k+1} = z_k + t_k$ are the respective distances from the midplane to the lower and upper surfaces of the k-t layer, t_k being the thickness of the layer.

Moreover, the constitutive equations for the k-th layer are:

$$\sigma_i^{(k)} = Q_{ij}^{(k)} \varepsilon_{ij}^{(k)} \tag{5}$$

where Q_{ij} are the stiffness coefficients of the k-th layer in the plate coordinates. From Eqs. 4 and 5 we obtain the plate constitutive equations:

$$\begin{Bmatrix} N_i \\ M_i \end{Bmatrix} = \begin{bmatrix} A_{ij} & B_{ij} \\ B_{ji} & D_{ij} \end{bmatrix} \begin{Bmatrix} \varepsilon_i^o \\ \chi_i \end{Bmatrix} \quad , \quad \begin{Bmatrix} Q_4 \\ Q_5 \end{Bmatrix} = \begin{bmatrix} \bar{A}_{44} & \bar{A}_{45} \\ \bar{A}_{45} & \bar{A}_{55} \end{bmatrix} \begin{bmatrix} \varepsilon_4 \\ \varepsilon_5 \end{bmatrix} \tag{6}$$

Here, the stiffness matrices: in-plane (A_{ij}), bending-in-plane coupling (B_{ij}), bending and twisting (D_{ij}), (i,j=1,2,6) and thickness shear (A_{ij}), (i,j=4,5) are given, respectively, by:

$$A_{ij} = \sum_k \int_{z_k}^{z_{k+1}} Q_{ij}^{(k)} dz \ , \quad B_{ij} = \sum_k \int_{z_k}^{z_{k+1}} Q_{ij}^{(k)} z dz \ , \quad D_{ij} = \sum_k \int_{z_k}^{z_{k+1}} Q_{ij}^{(k)} z^2 dz$$

$$\bar{A}_{ij} = \sum k_i \, k_j \int_{z_k}^{z_{k+1}} Q_{ij}^{(k)} dz \tag{7}$$

Referring back to eq. 3, q is the transverse distributed force; u_n, u_{ns}, ψ_n and ψ_s are the normal and tangential components of the in-plane displacements and rotations. Furthermore C_i are the portions of the boundary C of the midplane Ω on which $\bar{N}_n$, $\bar{M}_n$, $\bar{M}_s$, $\bar{Q}_n$, respectively, are specified.

DELAMINATION MODEL

A delamination model is now presented that is based on a unilateral contact concept where the adhesion between layers is modelled by elastic springs with finite tensile strength [12-15-16].

The spring reaction r depends on the elongation w (Fig. 2):

$$r(w) = \begin{cases} kw \text{ if } w \leq w_o \\ 0 \text{ if } w > w_o \end{cases} \tag{8}$$

where k is a positive constant.

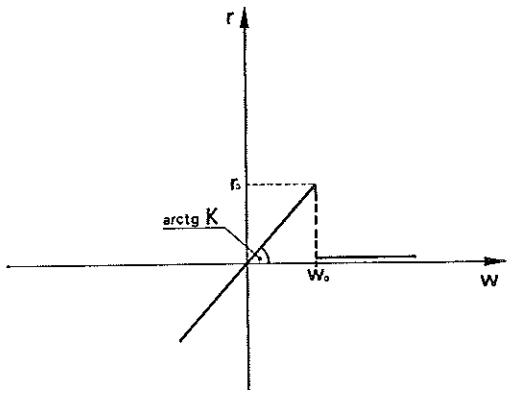

Fig. 2 - Unilateral Spring response.

Therefore, the spring strain energy cannot exceed $U_o = 1/2kw_o^2$ in tension. When the strain energy of the springs reaches U_o, the delamination of the layers is assumed to occur. The relation between U_o in the present approach and Γ in the fracture mechanics approach is given by $U_o = \Gamma$. Hence, the elongation limit w_o of the springs is given by:

$$w_o = \sqrt{\frac{2\Gamma}{k}} \tag{9}$$

For a given material, characterized by the strain energy limit U_o, it can be proven that when $k \to \infty$ the unilateral solution converges to the fracture mechanics solution.

The total potential energy of the plate is given by:

$$\bar{\Pi} = \Pi + \frac{1}{2}\int_{\Omega} k(w)\, w^2 \, d\Omega \tag{10}$$

Note that the second term on the right side of eq. (10) represents the contribution of the elastic response of the springs.

FINITE ELEMENT FORMULATION.

Let the region Ω be divided into a finite number of rectangular elements. Over each element the generalized displacements (u,v,w,ψ_x,ψ_y) are interpolated as follows:

$$u = \sum_{i=1}^{N} u_i f_i, \quad v = \sum_{i=1}^{N} v_i f_i, \quad w = \sum_{i=1}^{N} w_i f_i, \quad \psi_x = \sum_{i=1}^{N} \psi_{xi} f_i, \quad \psi_y = \sum_{i=1}^{N} \psi_{yi} f_i \tag{11}$$

where u , v , w , ψ_x , ψ_y are the values of the unknown functions at the N global nodes of the mesh and f_i are the global interpolation functions. The relevant governing equations of the nonlinear bending can be obtained by applying the stationary condition to the functional (3) in which displacements u,v,w,ψ_x,ψ_y are replaced by (11).

So, this gives the discrete form:

$$\underset{\sim}{K}\ \underset{\sim}{U} = \underset{\sim}{F} \tag{12}$$

where $\underset{\sim}{K}$ is the stiffness matrix, $\underset{\sim}{F}$ is the nodal force vector and $\underset{\sim}{U}$ collects the nodal values of the generalized displacements u, w ψ_x, ψ_y.

It should be observed that the stiffness matrix $\underset{\sim}{K}$ depends on the solution $\underset{\sim}{U}$. Therefore, a standard iterative procedure is used. As far as the buckling analysis is concerned, the total potential energy of the system is assumed to be of the form:

$$\Pi[u,\lambda] = \Phi(u) - \lambda \bar{p}\, u \tag{13}$$

where u, v, w, ψ_x, ψ_y is a generalized displacement field, $\Phi(u)$ is the strain energy given by the first integral on the right side of Eq. 3, and λ is a scalar parameter which determines the magnitude of the prescribed external loads p on the system.

As in [14], it is assumed that there exists a fundamental solution $\mu_o(\lambda)$ which satisfies the variational equation of equilibrium:

$$\Pi'[u_o(\lambda),\lambda]\ \delta u = \Phi'[u_o(\lambda)]\delta u - \lambda \bar{p}\, \delta u = 0 \tag{14}$$

The symbol ', above, denotes the Frechét derivative with respect to the displacements field u.

The variational equation governing the buckling, if bifurcation takes place, can be put into the form:

$$\Phi_c''\, u_1\ \delta u = 0 \tag{15}$$

where Φ_c'' stands for $\Phi''[u_o(\lambda_c)]$; λ_c and u_1 are, respectively, the buckling load and the buckling mode.

Eq. (11), by Eq. (8) becomes, in discrete form:

$$\underset{\sim}{H}[\underset{\sim}{U}_o(\lambda)]\ \underset{\sim}{U}_1 = \underset{\sim}{0} \tag{16}$$

where $\underset{\sim}{U}_o$ and $\underset{\sim}{U}_1$ collect the nodal values of the prebuckling displacement u_o, and of the buckling mode u_1, respectively. The tangential stiffness matrix $\underset{\sim}{H} = [H_{ij}]$, evaluated along the prebuckling path $\underset{\sim}{U}_o(\lambda)$, is defined by the relation:

$$H_{ij}\,[\underset{\sim}{U}_o(\lambda)]\delta U_i^{(1)}\ \delta U_j^{(2)} = \Phi''[u_o(\lambda)]\delta u^{(1)}\ \delta u^{(2)} \tag{17}$$

for all admissible $\delta u^{(1)}$, $\delta u^{(2)}$.

For the numerical applications relative to the delamination problem, a similar finite element model to the one above can also be developed.

It can be shown [12] that also in this case the stationary condition of the energy functional (10) leads to the following discrete equilibrium equation:

$$\bar{\underset{\sim}{K}}\ \underset{\sim}{U} = \underset{\sim}{F} \tag{18}$$

where $\underset{\sim}{U}$ collects the nodal values of u,v,w, etc., $\bar{\underset{\sim}{K}} = \underset{\sim}{K} + \underset{\sim}{K}_k$ is the stiffness matrix and $\underset{\sim}{F}$ is the force vector. It can be observed that the stiffness matrix $\bar{\underset{\sim}{K}}$ depends on the solution U, because of both the nonlinear strain-displacement relation (2) and the nonlinear reaction-deflection relationship of the springs.

Therefore, the solution of the unilateral contact problem can be obtained by solving a sequence of auxiliary bilateral problems in which the contribution $\underset{\sim}{K}_k$ of the springs at the h-th step sequence is evaluated (according to eq. (8)) from the displacement solution w_{h-1} of the previous bilateral problem.

More precisely, at the h-th step the matrix $\underset{\sim}{K}_k$ is evaluated as follows:

$$K_{k_{ij}}^{(h)} = \sum_{N_e} \sum_{N_G} k\, P_G^{(h)} f_i(x_e)\ f_j(y_e) \tag{19}$$

where N_G is the number of Gauss points of the e-th element and the coefficient $P_G^{(h)}$ are defined as:

$$P_G^{(h)} = \begin{cases} W_G \text{ (Gaussian weight at point } (x_e, y_e)) & \text{if } w^{(h-1)}(x_e, y_e) = f_i\ w_i^{(h-1)} < w_o \\ 0 & \text{if } w(x_e, y_e) = f_i\, w_i^{(h-1)} \geqslant w_o \end{cases} \tag{20}$$

Besides which, each of these bilateral problems are geometrically nonlinear and can be solved by a standard iterative procedure.

NUMERICAL RESULTS AND DISCUSSION

Formulations introduced so far, are then utilized in the nonlinear ana-

lysis of moderately thick rectangular plates. The following material properties, typical of advanced fiber reinforced composites, are considered:

MATERIAL I (M1) : $E_1=25E_2$, $G_{12}=G_{13}=0.5E_2$, $\nu_{12}=0.25$

MATERIAL II (GL) : $E_1=3E_2$, $G_{12}=G_{13}=G_{23}=0.6E_2$, $\nu_{12}=0.25$

MATERIAL III (GR) : $E_1=40E_2$, $G_{12}=G_{13}=G_{23}=0.5E_2$, $\nu_{12}=0.25$

MATERIAL IV (BO) : $E_1=10E_2$, $G_{12}=G_{13}=G_{23}=E_2/E_3$, $\nu_{12}=0.22$

MATERIAL V : $E_1=25E_2$, $G_{12}=G_{13}=G_{23}=0.5E_2$, $\nu_{12}=0.25$

E_1 and E_2 are, respectively, the layer elastic moduli in direction along fibers and normal to them, G_{12} - G_{13} and G_{23} are, respectively, the layer in-plane and thickness shear moduli, and ν_{12} is Poisson's ratio. In all calculations shear correction factors are assumed to be $K_4^2 = K_5^2 = 5/6$.

Moreover the following boundary conditions are considered:

a) SS1 (Simply supported)

$u(x,0) = u(x,b) = w(x,0) = w(x,b) = \psi_x(x,0) = \psi_x(x,b) = 0$

$v(0,y) = v(a,y) = w(0,y) = w(b,y) = \psi_y(0,y) = \psi_y(a,y) = 0$

b) CSCS (Simply supported)

$w(x,0) = w(x,b) = \psi_y(x,0) = \psi_y(x,b) = 0$

$w(0,y) = w(a,y) = \psi_y(0,y) = \psi_y(a,y) = v(0,y) = v(a,y) = 0$

c) CC1 (Clamped)

all edges clamped $u = v = w = \psi_x = \psi_y = 0$

d) CC2 (Clamped)

$w(x,0) = w(x,b) = w(y,0) = w(y,a) = 0$

$\psi_x(0,y) = \psi_x(a,y) = \psi_y(x,0)\ \psi_y(x,b) = 0$

e) SS2 (Simply supported)

$v(x,0) = w(x,0) = \psi_x(x,0) = 0$; $w(x,b) = \psi_x(x,b) = 0$

$u(0,y) = w(0,y) = \psi_y(0,y) = 0$; $w(a,y) = \psi_y(a,y) = 0$

NON LINEAR BENDING ANALYSIS

In this section some numerical results are presented concerning large deflection analysis of square and rectangular plates obtained with a mesh of F.E.M. 3x3 nine-node quadratic elements. It should be noticed that no appreciable effect of the integration of shear terms was observed in calculations for the quadratic elements used.

Fig. 3 plots the nondimensional transverse central deflection w_c/h versus the E_1/E_2 ratio for a simple supported (SS1) square plate. In particular the diagrams show the dependence of the coupling effect on the ratio E_1/E_2.

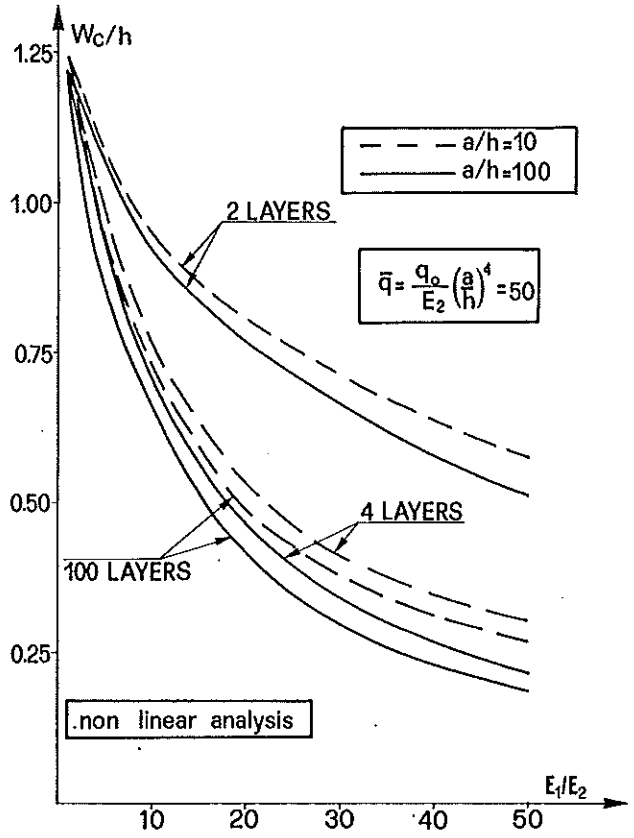

Fig. 3 - Square cross ply-plate under transverse load: maximum deflection v/s E_1/E_2 ratio.

A sufficiently high transverse nondimensional load $\bar{q} = (q_o/E_2)(a/h)^4$ was assumed, in order to have an appreciable influence of nonlinearities.

Thicknesses of all layers are assumed to be constant. The influence of shear deformability on nonlinear bending is pointed out again in Fig. 3, by the comparison of results relative to the ratios a/h = 100 and a/h = 10, respectively.

Fig. 4 shows the variation of the nondimensional center deflection versus the a/b aspect. It should be observed that the influence of coupling can be extremely relevant, although the center deflection rapidly reaches the uncoupled solution as the number of plies are increased. The influence of the shear deformability is confirmed by the different values of center deflection obtained for a/h = 10 and a/h = 100.

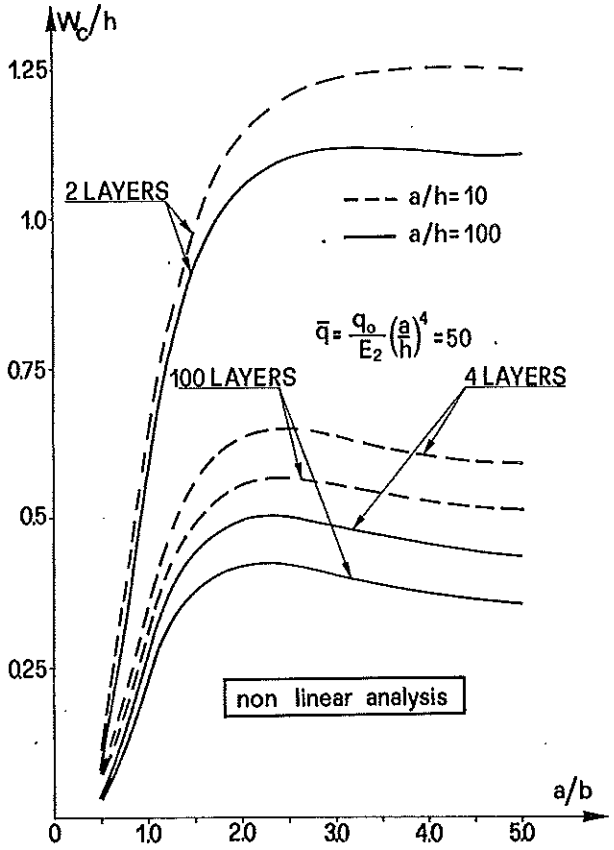

Fig. 4 - Center deflection v/s the aspect ratio a/b of a cross ply plate under transverse load.

Figs. 5 a,b,c shows the variation of the nondimensional center deflection

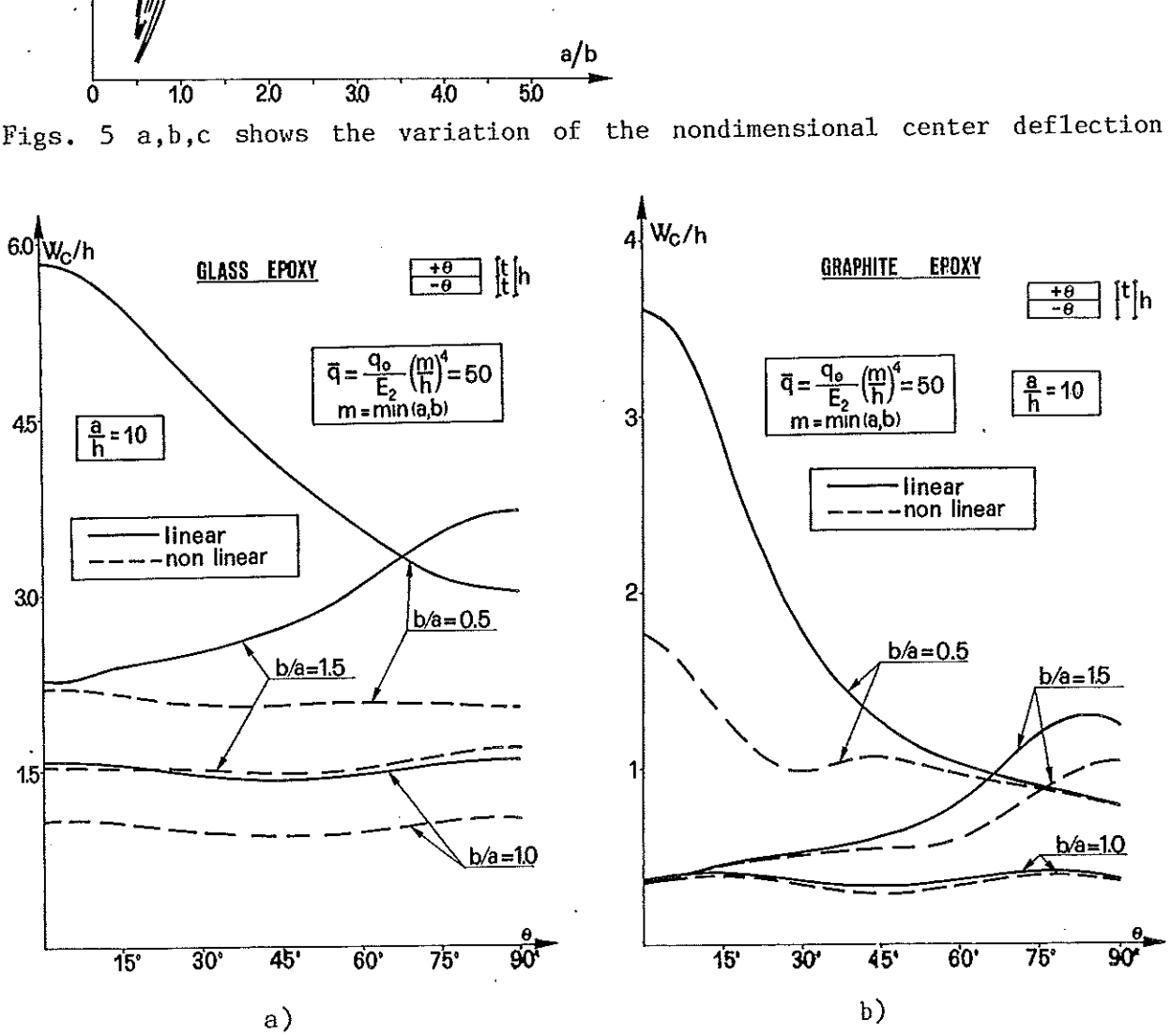

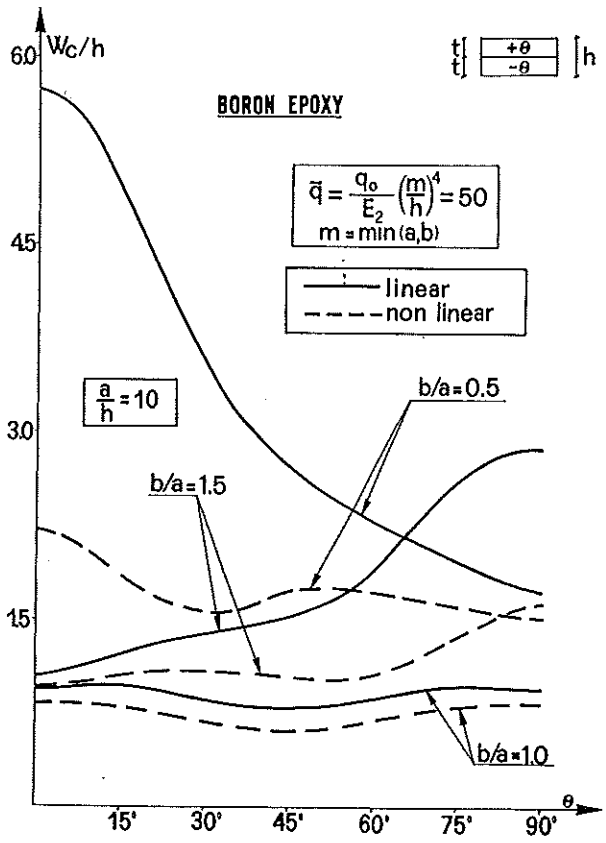

c)

Fig. 5 - Center deflection of two-layers plate v/s fiber orientation.

((w_c/h) with fiber orientation of a two layer angle-ply plate for various b/a ratios. Fig. 5a concerns a Glass-Epoxy laminate (material II), Fig. 5b is relative to a Graphite-Epoxy one (material III) and Fig. 5c considers a Boron-Epoxy laminate (material IV). In all cases the a/h ratio was fixed at 10 and the nondimensional load q was considered to be 50. As can be observed, there is a large difference between linear and nonlinear solutions.

Figs 6a, b shows the variation of the nonlinear to linear transverse displacement ratio versus $\bar{q} = (q_o/E_2)(a/h)^4$, under different boundary conditi-

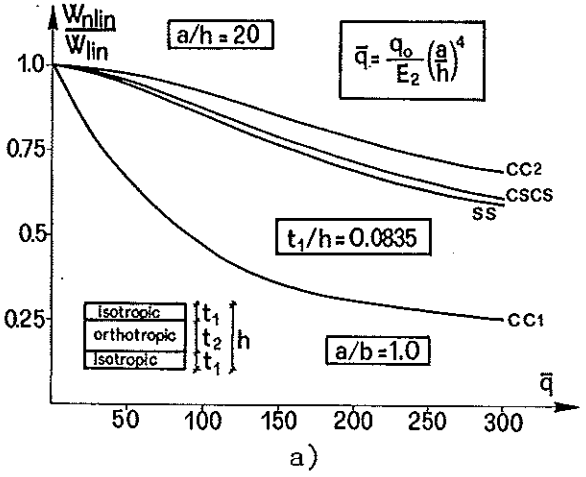

a)

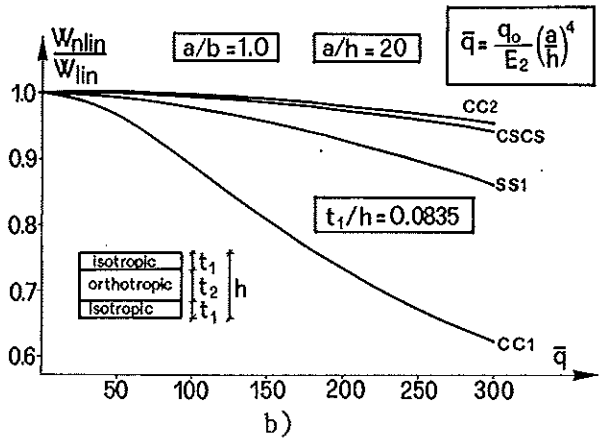

b)

Fig. 6 - Three-layered sandwich plate under transverse load: linear and non-linear bending ratio v/s undimensional load.

ons, for a three-layered sandwich plate.

The nonlinear effect increases with load; the effect of nonlinearity is at a minimum in CC2 boundary conditions while the maximum effect is found CC1 boundary conditions.

This is due to the inclusion in the CC1 boundary conditions of nonlinear terms in the strain displacement relations and the suppression of axial displacements which may have contributed to the maximum nonlinearity of the plate. Case (a) is different to case (b) regarding the value of Young's modulus of isotropic layers.

BUCKLING ANALYSIS

The first example considered here is an angle-ply square plate composed of material II, subject to biaxial uniform compression $N = N_x = N_y$ and under SS2 boundary conditions. This scheme was already considered in [13] in which the Kirchhoff-Love thin plate theory was used.

In Fig. 7, the nondimensional buckling load versus angle-ply orientation is plotted.

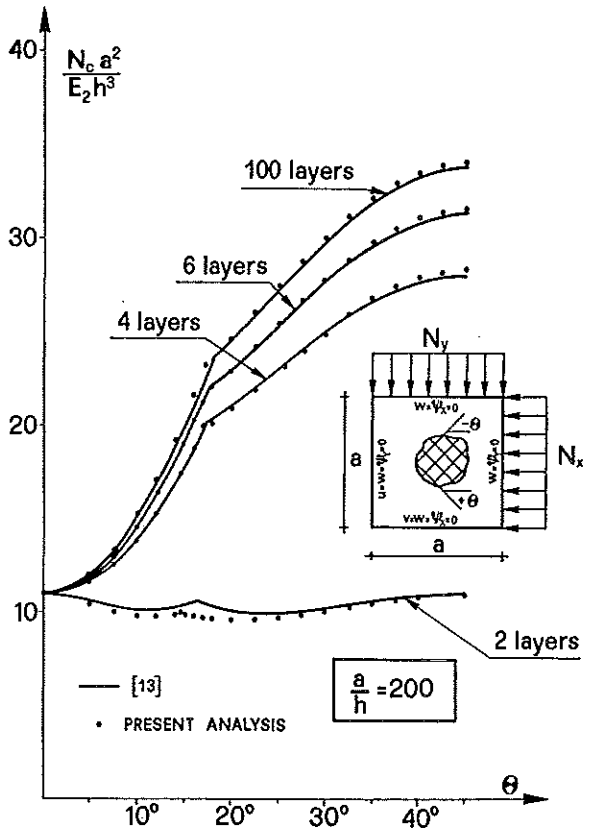

Fig. 7 - Angle-ply square plate (SS2 boundary condition, material II) under biaxial compression: critical buckling load v/s angle-ply orientation

Results are obtained by using a finite element computational procedure and compared to those of Ashton and Whitney [13]. As can be seen, the influence of coupling on buckling is very pronounced. In fact, when the number of layers is large, the "orthotropic" solution is attained, and higher values of the buckling load are reached, with an optimal value of the orientation angle: $\theta = 45°$.

On the other hand, for the two layer plate example the influence of coupling on buckling is strong, as shown in Fig. 7. In this case the agreement between analytical [13] and the F.E.M. results is less close than the "orthotropic" one, owing to the influence of the orientation angle on the shape of the buckling mode.

The second example considered in the buckling analysis, is devoted to focus the effect of the aspect ratio a/b. For this goal the behaviour of plates, composed of different materials and subject to uniform uniaxial compressive load, was analyzed.

In Fig. 8 the critical load N_x is plotted against the aspect ratio a/b; note that the buckling mode depends both on the a/b ratio and the material properties.

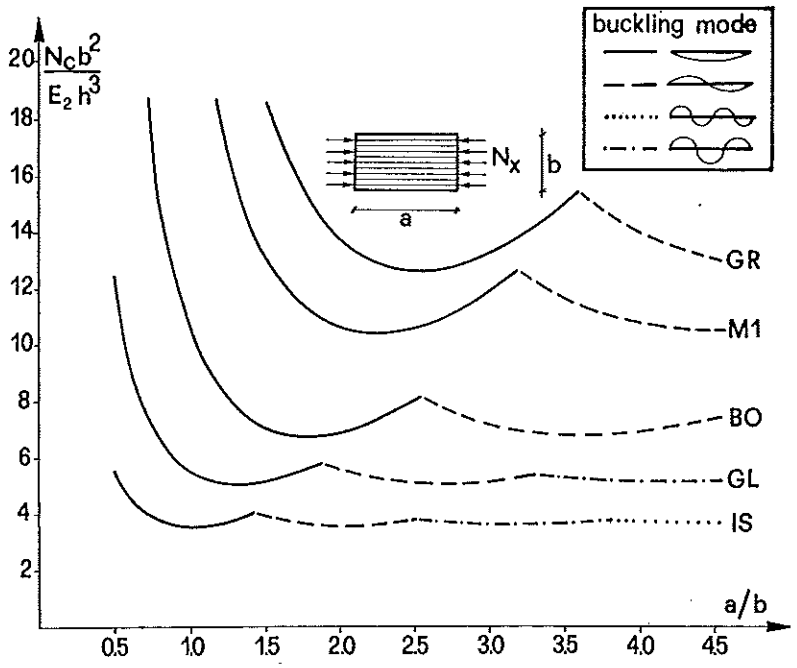

Fig. 8 - Variation of critical buckling load (uniaxial compression) with aspect ratio and material properties.

DELAMINATION ANALYSIS

Here, some numerical applications are developed starting from the analysis obtained in previous sections.

The plate model schemes are shown in Figs. 9a, b.

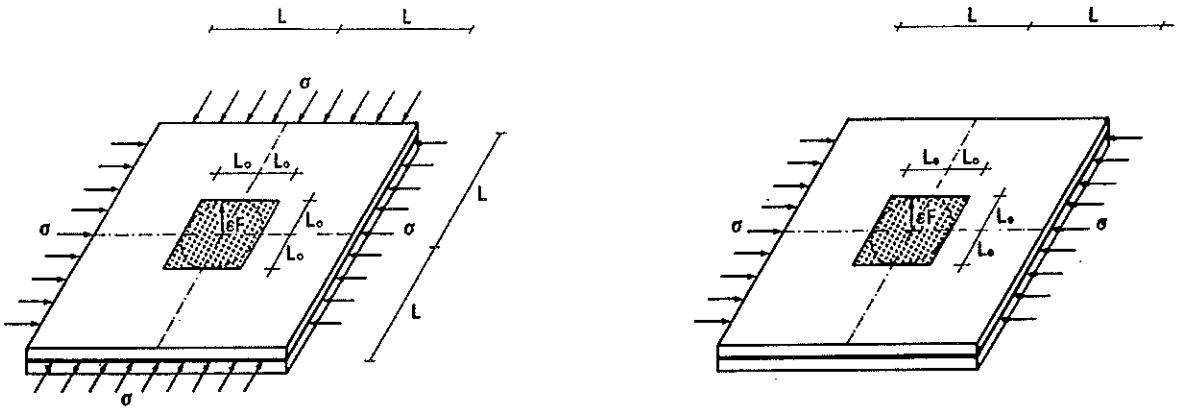

a) b)

Fig. 9 - Square plate example: (a) isotropic, (b) orthotropic.

The first scheme (Fig. 9a) refers to a square isotropic two-layer sandwich plate with an initial defect: square (side $2L_o$) or circular (radious L_o). The plate is subject to a uniform edge pressure σ and to a symmetrical (with respect to the x-y plane) transverse load imperfection εF, F being given by: $F=hD/4\alpha L^2$ (with $\alpha = 0.0056$).

The second scheme concerns an orthotropic square plate subject to a uniaxial edge load σ in the x direction and to a transverse load imperfection εF similar to that of the square isotropic plate.

In the application of the finite element technique, a higher accuracy is evidently required in the proximity of the delamination front.

Therefore, the finite element mesh refinement is limited to a plate region defined by a suitable value of the parameter L_1, with a sufficient number N_2 of mesh divisions beyond the delamination front as shown in Fig. 10. Due to symmetry, only a quarter of the plate is modelled.

Regarding the numerical applications, the values $N_o=4$, $N_1=10$, $N_e=18$, $L_1=5\lambda$ (with $\lambda = (4D/k)^{1/4}$ were adopted.

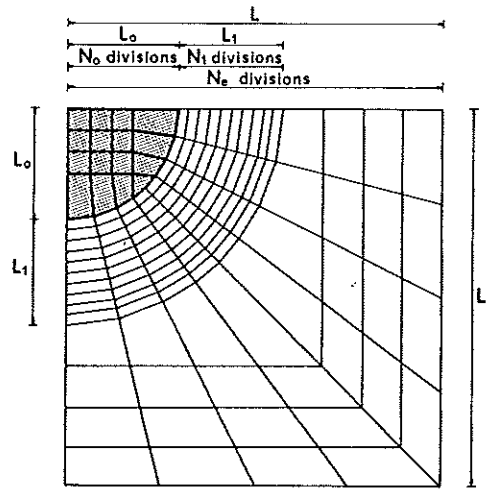

Fig. 10 - Finite element mesh of a plate with a circular bonding defect.

In Fig. 11a,b,c significant results are given; in particular the interlaminar tensile stresses r/r_o at the delamination front are plotted for given values of the adhesion energy parameter $\beta_o = \Gamma L^2/\sigma h^3$, where $\sigma = 4\pi^2 D/L^2 h$ is assumed. Results refer to cases of circular and square bonding defects both for isotropic and orthotropic plates, and are obtained by using the value $\tau = 10^{14}$ of the spring stiffness parameter $\tau = k L_o^4/D$ (D: flexural stiffness).

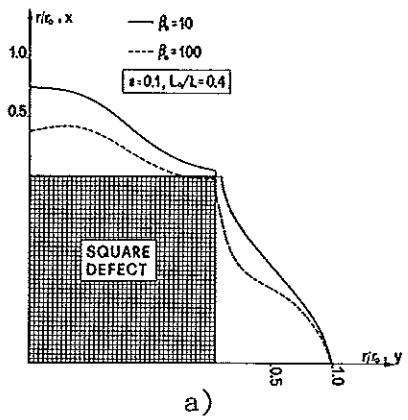

a)

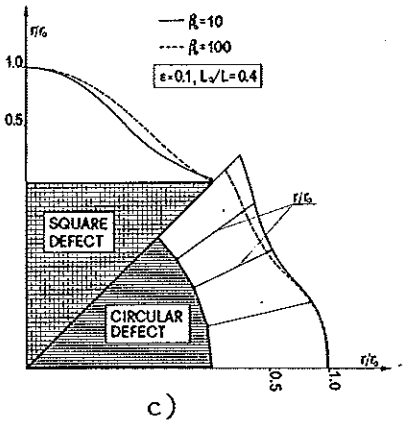

c)

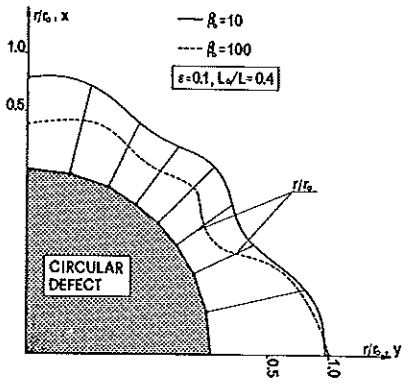

b)

Fig. 11 - Square plate example (h/L = 0.001): interlaminar normal stresses at the delamination front. (a), (b) orthotropic (MAT. II) (c) isotropic.

It is worth noting that the onset of delamination depends on the adhesion energy parameter β_o, particularly in the case of an orthotropic plate.

The third example presented concerns the delamination of a two-layer square plate of side a (Fig. 12) subject to transverse load F.

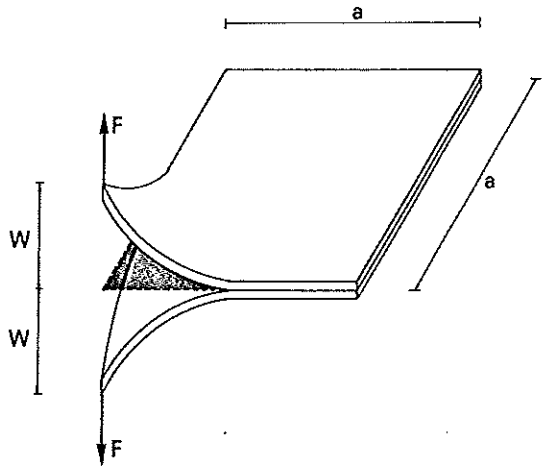

Fig. 12 - Delamination of a two-layer square plate.

The weld has an initially defective square portion of side L_o. Results showing the load-deflection relationship and the shape of the opening front are given in Fig. 13. The quantities W, L^* defined as:

$$W = \frac{3}{2}\frac{w_c}{L^*} \qquad L^* = \sqrt{\frac{2D}{U_o}} \tag{21}$$

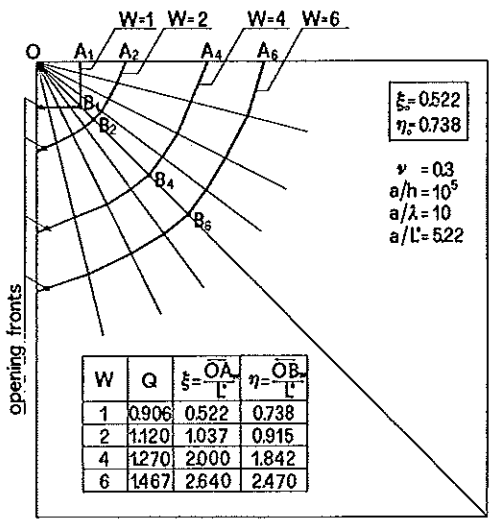

W	Q	$\xi=\frac{\overline{OA}}{L^*}$	$\eta=\frac{\overline{OB}}{L^*}$
1	0.906	0.522	0.738
2	1.120	1.037	0.915
4	1.270	2.000	1.842
6	1.467	2.640	2.470

Fig. 13 - Evolution of the opening front.

Finally in Fig. 14 some results relative to the delamination buckling of a symmetrically compressed two-layer isotropic narrow-plate are presented. In particular, a comparison between analytical results, obtained via fracture mechanics, and those obtained by the F.E.M. unilateral contact approach is shown. A fair agreement can be observed between the two approaches when high values of the spring penalty parameter $\tau = k\ell_o^4/D$ are used.

From previous results it can be concluded that the proposed F.E.M. analysis represents an efficient tool for studying two-dimensional problems, where the fracture mechanics approach is harder to apply.

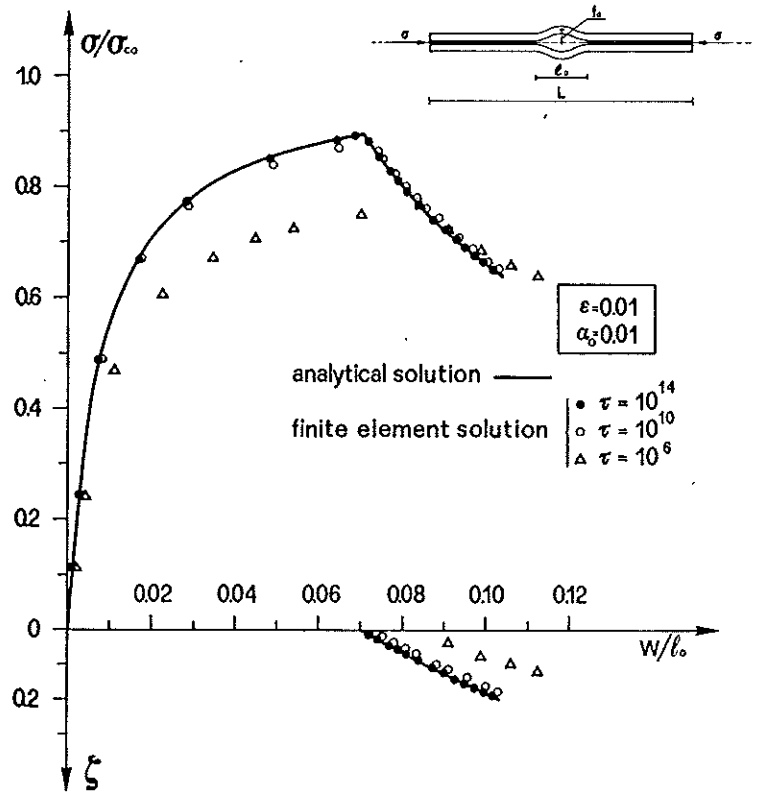

Fig. 14 - Symmetric narrow-plate model with initial imperfection $\varepsilon = f_o/\ell_o$. Central transverse deflection w v/s nondimensional applied load σ/σ_{co} , and delamination parameter $\zeta = \ell/\ell_o - 1$.
$\sigma_{co} = 4\pi^2 D/\ell_o^2$: local buckling load;
ℓ : actual opening length;
$\alpha_o = 4\Gamma\zeta/\pi^2\sigma_{co}$: adhesion energy parameter.

REFERENCES

[1] E. Reissner and Y. Stavsky, Bending and stretching of certain types of heterogeneous aeolotropic elastic plates, J. Appl. Mech. 28, 402-408 (1961).

[2] C.W. Bert and B.L. Mayberry, Free vibrations of unsymmetrically laminated anisotropic plate with clamped edges, J. Composite Materials 3, 282-293 (1969).

[3] N.J. Pagano, Exact solution for composite laminates in cylindrical bending, J. Composite Materials 3, 398-411 (1969).

[4] N.J. Pagano and S.J. Hatfield, Elastic behaviour of multilayer bi-directional composites, AIAA J. 10, 931-933 (1972).

[5] C.W. Bert and T.L. Chen, Effect of shear deformation on vibration of antisymmetric angle-ply laminated rectangular plates, Int. J. Solids and Structures 14, 465-473 (1978).

[6] J. N. Reddy, Free vibration of antisymmetric angle-ply laminated plates, including transverse shear deformation by the finite element method, J. Sound Vib. 66 (4), 565-576 (1979).

[7] P.C. Yang, C.H. Norris and Y. Stavsky, Elastic wave propagation in heterogeneous plates, Int. J. Solids and Structures 2, 665-684 (1966).

[8] J.M. Whitney and N.J. Pagano, Shear deformation in heterogeneous anisotropic plates, J. Appl. Mech. 37, 1031-1036 (1970).

[9] J.M. Whitney and A.W. Leissa, Analysis of heterogeneous anisotropic plates, J. Appl. Mech. 36, 261-266 (1969).

[10] S.A. Zaghloul and J.B. Kennedy, Non-linear analysis of unsymmetrically laminated plates, J. Engng. Mech. Div. ASCE 101 (EM3), 169-185 (1975).

[11] J.N. Reddy and W.C. Chao, Non-linear bending of thick rectangular laminated plates, Int. J. Non-linear Mech., Vol. 16, N° 314, 291-301, (1981).

[12] L. Ascione, and D. Bruno, On the delamination of two-layer plates, Proc. Second Meeting on Unilateral Problems in Structural Analysis, Ravello (1983). CISM Courses and Lectures n. 288, Springer-Verlag, Wien-Berlin.

[13] J.E. Asthon and J.M. Whitney, Theory of laminated plates, Technomic Publication, (1970).

[14] B. Budiansky, Theory of buckling and postbuckling behaviour of elastic structures, in Advances in Applied Mechanics, Vol. 14, ed. by Chia-Shun Yih, Academic Press, New York (1974).

[15] D. Bruno, Delamination buckling in composite laminates with interlaminar defects, Theoretical and Applied Fracture Mechanics 9, 145-159 (1988).

[16] D. Bruno, A. Leonardi and G. Porco, An analysis of delamination in laminated composite plates, IX Congresso AIMETA, Vol. II, 497-500, Bari, (1988).